Chapter 4

High resolution microparticle profiles at NGRIP: Case studies of the calcium – dust relationship

Urs Ruth, Dietmar Wagenbach, Matthias Bigler, Jørgen P. Steffensen, Regine Röthlisberger, and Heinz Miller

Annals of Glaciology, Volume 35 (2002), in press

High resolution microparticle profiles at NGRIP: case studies of the calcium - dust relationship

Urs Ruth[1,2], Dietmar Wagenbach[1], Matthias Bigler[3], Jørgen P. Steffensen[4], Regine Röthlisberger[3], and Heinz Miller[2]

[1]Institut für Umweltphysik, University of Heidelberg, Germany
[2]Alfred Wegener Institut für Polar- und Meeresforschung, Bremerhaven, Germany
[3]Climate and Environmental Physics, University of Bern, Switzerland
[4]Department of Geophysics, University of Copenhagen, Denmark

Annals of Glaciology, Volume 35 (2002), in press

ABSTRACT

A novel flow-through microparticle detector was deployed concurrently with continuous flow analyses of major ions during the NGRIP 2000 field season. The easy handling detector performs continuous counting and sizing. In this deployment the lower size detection limit was conservatively set to 1.0 μm equivalent spherical particle diameter, and a depth resolution of $\leq$ 1 cm was achieved for microparticle concentrations. The dust concentration usually followed the Ca^{2+} variability. Here results are presented from an inspection of the Ca/dust mass ratio in 23 selected intervals, 1.65m long each, covering different climatic periods including Holocene and last glacial maximum (LGM). A (Ca^{2+})/(insoluble dust) mass ratio of 0.29 was found for Holocene and 0.11 for LGM. Changes of the Ca/dust ratio also occur on an annual to multi-annual time scale exhibiting the same pattern, i.e. a lower Ca/dust ratio for higher crustal concentrations. Moreover, the Ca^{2+}/dust ratio may increase significantly during episodic events such as volcanic horizons due to enhanced dissolution of $CaCO_3$. This questions the notion of deploying Ca2+ as a quantitative mineral dust reference species and stresses the importance of variable source properties or fractionating processes during transport and deposition.

INTRODUCTION

The atmospheric mineral dust load, mainly composed of insoluble mineral particles, is an important part of Earth's climatic system as it is involved in direct and indirect radiative forcing processes (e.g. Tegen and Fung, 1994). Equally, the amount, size distribution and composition of dust deposited on polar ice sheets may hold valuable information about both, positions and climatic conditions of source areas, as well as about long range transport and deposition processes (Biscaye and others, 1997; Fuhrer and others, 1999). Over the last climatic cycle, Greenland as well as Antarctic mineral dust records exhibit changes on a huge dynamic range (e.g. Hansson, 1994; Steffensen, 1997; Petit and others, 1999). In Greenland these changes occurred very rapidly and were coinciding with changes in $\delta^{18}O$ at rapid climatic transitions within the last Pleistocene as has been inferred from high resolution measurements of Ca^{2+} and ECM on the GRIP and GISP2 ice cores (Taylor and others, 1997; Fuhrer and others, 1999).

The concentration of Ca ions (Ca^{2+}) is often being used as a proxy parameter for total mineral dust in ice cores as it represents the major part of the readily dissolved fraction of the dust aerosol. But the soluble proportion of dust is not constant over different climatic periods (Steffensen, 1997), so using Ca^{2+} as a proxy may give a distorted view of the total dust concentration. However, also dust measurement techniques have specific disadvantages. Only low resolution profiles or selected continuous sections have been measured for insoluble microparticles using the well established Coulter counting technique (e.g. Steffensen, 1997) because it requires extensive sample preparation and handling. And high resolution continuous dust measurements using 90° laser light scattering off melt water (Hammer and others, 1985) or off ice (Ram and Koenig, 1997) yield no size distribution information or are difficult to calibrate.

Here we introduce a novel laser sensor device for microparticle measurements deployed for continuous recordings of microparticle concentration and size distribution during the North Greenland Ice Core Project (NGRIP) 2000 field season. Apart from the methodical aspects, we present and discuss case studies of the dust concentration focussing on the Ca^{2+}/dust ratio under inconspicuous conditions as well as in volcanic horizons.

EXPERIMENTAL SETUP

During the NGRIP 2000 field season, extensive scientific processing was performed shortly after retrieval of the ice core. This included the operation of a warm laboratory for continuous flow analyses (CFA) of Ca^{2+}, Na^{+}, NH_4^{+}, SO_4^{2-}, NO_3^{-}, H_2O_2 and HCHO concentrations, and of electrolytical conductivity (Röthlisberger and others,

2000). Concurrently, continuous microparticle counting and sizing was performed. Discrete liquid samples were collected at 55 cm resolution for subsequent ion chromatography (IC) analysis; and over selected depths, discrete samples for IC and acidity measurements at approx. 6 cm resolution were also collected by an automatic sampler. The contamination free sample water for all these analyses was drawn from the inner area of a melt head, where the ice was melted at approx. 4 cm min^{-1}. For an overview of the setup see Figure 1. By these means the core was continuously analyzed from approx. 1400 m to 2930 m depth.

The particle sensor

The particle sensor, for general purpose laboratory applications, is from Klotz GmbH, Bad Liebenzell, Germany, and was specifically modified in collaboration with the Institut for Environmental Physics of the University of Heidelberg (Saey, 1998; Armbruster, 2000). The sample water is pumped through the detection cell, where it is illuminated by a 1.5 μm by 250 μm wide laser light beam of 670 nm wavelength. The transmitted light is measured by a photo diode detector (see Figure 2). When a particle passes through the detection area the transmitted light is attenuated by shadowing and scattering which results in a negative peak of transmitted light. The peak is counted and sorted by height into 32 bins, that can be adjusted to appropriate size intervalls.

The inter-relation of peak height and particle size is complex. Geometric shadowing is combined with scattering processes, both depending not only on particle volume but also on particle shape, material and orientation. A size calibration was achieved by measuring NGRIP ice core samples from different climatic periods with a Coulter counter and tying the laser sensor measurements of identical depths to the Coulter counter spectra. The calibration measurements showed the particle detection limit to be approx. 0.8 μm of spherical equivalent particle diameter. For our measurements, we used 1.0 μm diameter as the lower detection limit to be safely above the level of detector noise.

In our measuring procedure, size distributions were averaged over 1.65 m intervals. Respective results including size calibration will be presented elsewhere (Ruth, in preparation). The bulk particle number concentration was obtained continuously. To do so, the momentary count rate, converted to an analogue output signal, was recorded and the flow rate regularly measured. The continuously recorded data was later reduced to 1 mm depth intervals. Dust mass concentrations were inferred by integrating the particle size distributions that were obtained for each 1.65 m section and a material density of 2.7 g cm^{-3}; on average, this yielded that 1000 count ml^{-1} are equivalent to 5.6 μg kg^{-1}. For each section, the relative error of particle mass is about 15% due to size calibration uncertainties and varying pump rates.

To avoid coincidence distortion of the measurements the output signal is cut off by the counter electronics if the counting rate exceeds 4000 particles s^{-1}, so the sample flow needs to be decreased for high particle concentrations. However, as flow rates below 1 ml min^{-1} increase the sample dispersion in the flow system, the sample water from glacial age ice, which has a considerably higher dust concentration, was diluted with 0.2 μm prefiltered carrier water. Hereby an effective sample flow of approx. 0.15 ml min^{-1} could be established while keeping the flow through the sensor above 2 ml min^{-1}. The dilution setup allowed for measuring concentrations lower than 15 $\mu g\ kg^{-1}$ and in excess of 15,000 $\mu g\ kg^{-1}$, thus, covering the full dynamic range from Holocene to last glacial maximum (LGM). When used without the dilution system, the detection limit in terms of minimal count rate was about 200 particles ml^{-1}; this value however is dependent on the flow rate.

As used in our setup, the depth resolution of the microparticle measurement – expressed as the observed 1/e-depth of a step signal – is $\leq$ 1 cm. It is generally similar to the depth resolution of most other CFA-components, often slightly better. Apart from the melt rate, the depth resolution is limited by the conical surface of the melt head, by dead volumes and by longitudinal sample dispersion in the flow system. The impairment in depth resolution from using the dilution system was around 10%. In ice with low particle concentration, the counting statistics also impose a limit on the depth resolution by raising the error of a data point if the number of counts for this data point is low, thus, demanding an increase of interval width for each data point. However, the contribution of this statistical effect is more than one order of magnitude less than that of the mentioned physical factors.

Microparticle concentrations are reported here for the size fraction from 1.0 μm to 11.5 μm equivalent spherical diameter in $\mu g\ kg^{-1}$. The mass fraction not measured below 1.0 μm accounts for about 10% assuming a typical lognormal volume distribution.

List of samples

From the whole NGRIP core profile 23 sections, each 1.65 m long, are taken for this study. These sections cover depths from 1420 m to 2921 m and represent various climatic periods including Holocene and LGM. For all sections $\delta^{18}O$ data are already available (personal communication from NGRIP members, 2000). For some sections acidity and standard IC anion data is also available and will be included in our discussion. Table 1 gives an overview of all selected sections, many of which contain volcanic horizons.

RESULTS AND DISCUSSION

A: The high resolution profiles

Articulate variations of the dust concentration are observed throughout large sections of the core. Figure 3 shows two 1.65 m long sections of the microparticle and Ca^{2+} profiles, one out of the Holocene and one out of the LGM. Typical peak heights for microparticles are about 6 times (Ca^{2+}: 4 times) the background value in the Holocene and about 2.2 times (Ca^{2+}: 2.0 times) in the LGM section. Based on a preliminary estimate of annual layer thicknesses λ, which was done by applying the GRIP ages from Johnson and others (1997) to identified horizons in the NGRIP core, we expect that the variations may correspond to annual variations in the Holocene section; in the LGM section partly annual and partly multi-annual variations may be resolved. The insoluble dust profile, therefore, may assist the dating by annual layer counting based on other high resolution profiles, such as ECM, Ca^{2+}, Na^{+}, or visual stratigraphy (e.g. Meese and others, 1997).

B: Variation of the Ca^{2+}-to-dust ratio

Normally, a good correspondence is observed between insoluble microparticle and Ca^{2+} concentrations for Holocene ice as well as for glacial age ice. The correlation coefficients for the two examples shown in Figure 3 are 0.92 (Holocene) and 0.89 (LGM) after slight smoothing of both signals (see below). A similarly high correlation is found throughout the whole core. This at first sight may be seen as a general confirmation for the use of Ca^{2+} concentrations as a proxy for the insoluble mineral dust variability.

A more detailed examination of the Ca^{2+}/dust ratio reveals, however, distinct differences between the Holocene and the glacial section. To inspect these, the Ca^{2+}/dust ratio was calculated for each data point and smoothed to weaken artifacts arising from incorrect peak phasings and from different peak shapes caused by signal noise, different sample dispersion or different response characteristics of the two detection systems. For the smoothing a 5.0 cm wide hanning window was used, i.e. a gliding average using a cosinusoidal weighting function. The smoothed Ca^{2+}/dust ratio is included in Figure 3. It varies significantly on the same depth scale as peaks occur in the crustal concentrations and tends to be enhanced during low dust levels. The (mean Ca^{2+}) / (mean dust) ratio of the two sections are ~ 0.29 for Holocene and ~ 0.11 for LGM, which is similar to earlier findings from Steffensen (1997) based on established Coulter counter and standard IC measurements.

For all ice core sections listed in Table 1 the Ca^{2+}/dust mean ratios were calculated; hereby horizons with strong acid inputs, that showed unusually high Ca^{2+}/dust values (see below), were excluded. Figure. 4 shows the such derived (mean Ca^{2+}) / (mean dust) ratios plotted against $\delta^{18}O$; mean microparticle concentrations are also shown. A gradual trend to lower mean ratios for isotopically colder samples is exhibited. It can be excluded that the observed trend is an artifact arising from possibly higher relative errors of the measurements for isotopically warmer samples, which have lower concentrations of Ca^{2+} and dust; even Holocene concentrations are well above detection limit, and both systems responded very linearly to sample concentrations. Also the Ca^{2+} fraction derived from sea salt aerosol does not contribute significantly.

In order to compare the measured R_0 = (Ca^{2+})/(insoluble dust) ratios with data on the elemental composition of airborne mineral dust or source material, the ratios R_0 need to be converted to R = (total Ca) / (total dust). It is: $R = a\frac{1}{(bR_0)^{-1} + c}$, where a = (total Ca) / (Ca^{2+}) ≈ 1 is the ratio of total Ca to dissolved Ca^{2+}, $b \approx 0.9$ is the correction for the dust fraction not measured below 1.0 μm, and $c = 2.5$ is the mass ratio of $CaCO_3$ to Ca, assuming that the dissolved dust fraction predominantly consisted of $CaCO_3$ or of species with similar mass. This approximation yields ratios of 0.16 for Holocene and 0.08 for LGM. This Holocene value is in weak agreement with a mean ratio of 0.09 (range: 0.06 – 0.18) deduced from measurements of total Ca and Al in recent Greenland firn by atomic absorption spectroscopy (Boutron, 1978), but it is larger than the value of 0.05 deduced from total Ca and Al analyses in Summit aerosol by Colin and others (1997). For comparison to both references, the reported Al masses were used to infer the total dust mass by assuming a crustal abundance of 8%.

The trend to lower observed values of Ca^{2+}/dust for lower $\delta^{18}O$ remains under dispute as several explanations may be invoked. These include possible changes of source areas and properties, or of fractionating transformation and removal processes during long range transport or deposition (e.g. Hansson, 1994; Wurzler and others, 2000). The observed effect may also possibly be explained by slower dissolution of Ca^{2+} due to alkaline conditions of glacial ice, which would lead to lower observed Ca^{2+} concentrations by the immediate CFA-detection method used here.

Changes of mineral dust source areas are a controversial topic in the literature. De Angelis and others (1997) – by comparing their Ca^{2+}/Mg^{2+} ratios to Bowen (1979) – deduce mean sediment sources for present day and marine carbonate sources for the last glacial. Biscaye and others (1997) – based on mineralogical and isotopic studies – propose no significant change of source area during times of variable dust fluxes within the last glacial. Hinkley and others (1997) – on the basis of mineralogical studies – presume a present day tropospheric background aerosol uniformly composed of average

crustal rock and not of carbonates. Maggi (1997) finds that weathering processes may have been changed with climate; but little is known about how this might have affected the relative abundances of $CaCO_3$ or $CaSO_4$ in the dust aerosol (Pye, 1987). A comparison of our data with Ca abundances in crustal material (Bowen, 1979) (see Table 2) suggests that marine carbonates or limestone sediments could have contributed significantly only during Holocene and that that during LGM mean crust and other sediments would have dominated. Various soils could have contributed at all times.

In the data presented here, it may be noteworthy that the variations of the Ca^{2+}/dust ratio that occur on an annual to multi-annual scale follow the same pattern as the variations just discussed on a long time scale. As can be seen in Figure 3 the Ca^{2+}/dust ratio is small during large dust concentrations, which at least for the Holocene may be driven by variability in the transport efficiency as known for the Arctic Haze phenomenon (Rahn and Borys, 1977). It seems possible that also on an annual time scale these variations may be attributed to changing source areas or may be closely linked to changing fractionation processes during long range transport.

C: Special events in the microparticle and Ca^{2+} profiles

Figure 5 shows an example of a 1.65 m long section from the time between GRIP interstadials 1 and 2 which exhibits several anomalies (denoted by $\alpha - \delta$). Event α is a strong dust layer (note that the microparticle concentration got cut off by the detector electronics). Event δ is an increase of the Ca^{2+}/dust ratio caused by a Ca^{2+} peak that has no corresponding microparticle peak; only NO_3^- exhibits a pronounced peak that may be related (e.g. Wolff, 1984). Events β and γ arise from two very strong Ca^{2+} peaks coinciding with only small insoluble dust peaks; they have a Ca^{2+}/dust ratio about 100% and 200% higher than the typical value. Coinciding are very strong peaks in SO_4^{2-} and also enhancements of ECM, acidity, and F^- (not shown) indicating volcanic horizons. These phenomena were observed during cold glacial times predominately, but they also occured during warm interstadials.

From our size distribution measurements we can rule out that the observed increase of the Ca^{2+}/dust ratio during events β and γ is only an artifact resulting from a dust size distribution severely shifted towards larger particles during these events. High inputs of acid however may lead to enhanced Ca^{2+}/dust ratios by promoting the rapid dissolution of calcite particles or $CaCO_3$ coatings. Indeed, all 13 anomalous Ca^{2+}/dust enhancements investigated in this study are accompanied by a clear SO_4^{2-} peak, indicating a strong input of acid (see Table 1).

An ionic balance was evaluated using major ion concentrations and acidity data for 10 of these sections, and it was found to be rather constant – not zero, at a low μeq

kg^{-1} level – across the disturbed horizons, which indicates that no unmeasured ionic species contributed substantially during these events. From the ionic balance, of course, it still cannot be distinguished to which extent SO_4^{2-} derived from H_2SO_4 or from mineral $CaSO_4$. But it seems much more probable that during volcanic events the predominant part of SO_4^{2-} originates from volcanic H_2SO_4 and that the Ca^{2+} peak is produced by enhanced dissolution of $CaCO_3$ during in-cloud processing or pre-analytical sample melting.

CONCLUSIONS

The novel particle sensor proved to be a reliable tool even under field conditions; it provided the total particle concentration at ≤ 1 cm depth resolution backed up by size distribution information. Thus, calibrated records of insoluble particle mass concentrations are obtained. Variations of the Ca/dust mass ratio were seen during long term climatic changes as well as on annual or multiannual time scales. This suggests variable source properties or variable fractionation during transfer, which should be investigated in more detail. If Ca^{2+} measurements are used as a quantitative proxy for mineral dust care must be taken when considering data across climatic transitions, at volcanic horizons, or at subseasonal resolution.

A dedicated investigation of Ca ion solubility in glacial meltwater and its implications for the CFA and IC analytical methods is essential as we are currently limited in our interpretation by this uncertainty. To elucidate possible variations in dust source areas and properties, or of changes in fractionation processes during long range transport, routine analysis of crustal reference elements like Al are needed as they would help to infer the total – i.e. soluble and insoluble – crustal concentration.

ACKNOWLEDGEMENTS

The North-GRIP project is directed and organised by the Department of Geophysics at the Niels Bohr Institute for Astronomy, Physics and Geophysics, University of Copenhagen. It is being supported by funding agencies in Denmark (SNF), Belgium (NFSR), France (IFRTP and INSU/CNRS), Germany (AWI), Iceland (RannIs), Japan (MECS), Sweden (SPRS), Switzerland (SNF) and the United States of America (NSF). We wish to thank all the funding bodies and field participants. Chris Zdanowicz is thanked for his helpful comments to improve the manuscript.

REFERENCES

Armbruster, M., 2000, *Stratigraphical dating of high alpine ice cores over the last 1000 years (in German)*, M.Sc. thesis, Institut für Umweltphysik, University of Heidelberg, Heidelberg.

Biscaye, P. E., F. E. Grousset, M. Revel, S. Van der Gaast, G. A. Zielinski, A. Vaars, and G. Kukla, 1997, Asian provencance of glacial dust (stage 2) in the Greenland Ice Sheet Project 2 Ice Core, Summit, Greenland, *Journal of Geophysical Research*, 102 (C12), 26765-26781.

Boutron, C., 1978, *Influences of aerosols of natural and antropogenic origin on the chemistry of polar snows (in French)*, Ph.D thesis, , University of Grenoble, Grenoble.

Bowen, H. J. M., 1979, *Environmental Chemistry of the Elements*, Academic Press, London.

Colin, J. L., B. Lim, E. Herms, F. Genet, E. Drab, J. L. Jaffrezo, and C. I. Davidson, 1997, Air-to-snow mineral transfer - crustal elements in aerosols, fresh snow and snowpits on the Greenland ice sheet, *Atmospheric Environment*, 31 (20), 3395-3406.

De Angelis, M., J. P. Steffensen, M. Legrand, H. Clausen, and C. Hammer, 1997, Primary aerosol (sea salt and soil dust) deposited in Greenland ice during the last climatic cycle: Comparison with east Antarctic records, *Journal of Geophysical Research*, 102 (C12), 26681-26698.

Fuhrer, K., E. W. Wolff, and S. J. Johnsen, 1999, Timescales for dust variability in the Greenland Ice Core Projct (GRIP) ice core in the last 100,000 years, *Journal of Geophysical Research*, 104 (D24), 31043-31052.

Hammer, C. U., H. B. Clausen, W. Dansgaard, A. Neftel, P. Kristinsdottir, and E. Johnson, 1985, Continuous impurity analysis along the Dye 3 deep core, in C.C.J. Langway, H. Oeschger, and W. Dansgaard (Eds.) *Greenland Ice Core: Geophysics, Geochemistry, and the Environmentl*, Geophysical Monograph 33, American Geophysical Union, Washington, 90-94.

Hansson, M. E., 1994, The Renland ice core. A Northern Hemisphere record of aerosol composition over 120,000 years, *Tellus*, 46B, 390-418.

Hinkley, T., F. Pertsiger, and L. Zavjalova, 1997, The modern atmospheric background dust load: recognition in Central Asian snowpack, and compositional contraints, *Geophysical Research Letters*, 24 (13), 1607-1610.

Johnsen, S. J., H. B. Clausen, W. Dansgaard, N. S. Gundestrup, C. U. Hammer, U. Andersen, K. K. Andersen, C. S. Hvidberg, D. Dahl-Jensen, J. P. Steffensen, H. Shoji, A. E. Sveinbjörnsdòttir, J. W. C. White, J. Jouzel, and D. Fisher, 1997, The $d^{18}O$ record along the Greenland Ice Core Project deep ice core and the problem of possible Eemian climatic instability, *Journal of Geophysical Research*, 102 (C12), 26397-26410.

Maggi, V., 1997, Mineralogy of atmospheric microparticles deposited along the Greenland Ice Core Project ice core, *Journal of Geophysical Research*, 102 (C12), 26725-26734.

Meese, D. A., A. J. Gow, R. B. Alley, G. A. Zielinski, P. M. Grootes, M. Ram, K. C. Taylor, P. A. Mayewski, and J. F. Bolzan, 1997, The Greenland Ice Sheet Project 2 depth-age scale: Methods and results, *Journal of Geophysical Research*, 102 (C12), 26411-26423.

Petit, J. R., J. Jouzel, D. Raynaud, N. I. Barkov, J.-M. Barnola, I. Basile, M. Bender, J. Chappellaz, M. Davis, G. Delaygue, M. Delmotte, V. M. Kotlyakov, M. Legrand, V. Y. Lipenkov, C. Lorius, L. Pépin, C.

Ritz, E. Saltzmann, and M. Stievenard, 1999, Climatic and atmospheric history of the past 420,000 years from the Vostok ice core, Antarctica, *Nature*, 399, 429-436.

Pye, K., 1987, *Aeolian dust and dust deposits*, Academic Press, London.

Rahn, K. A., and R. D. Borys, 1977, The Asian source of Arctic haze bands, *Nature*, 268, 713-715.

Ram, M., and G. Koenig, 1997, Continuous dust concentration profile of pre-Holocene ice from the Greenland Ice Sheet Projct 2 ice core: Dust stadials, interstadials, and the Eemian, *Journal of Geophysical Research*, 102 (C12), 26641-26648.

Röthlisberger, R., M. Bigler, M. Hutterli, S. Sommer, and B. Stauffer, 2000, A technique for contiunuous high resolution analysis of trace substances in firn and ice cores, *Environmental Science & Technology*, 34, 338-342.

Saey, P., 1998, *Concentration and size distribution of microparticles in alpine and polar ice cores (in German)*, M.Sc. thesis, Institut für Umweltphysik, University of Heidelberg, Heidelberg.

Steffensen, J. P., 1997, The size distribution of microparticles from selected segments of the Greenland Ice Core Project ice core representing different climatic periods, *Journal of Geophysical Research*, 102 (C12), 26,755-726,763.

Taylor, K. C., R. B. Alley, G. W. Lamorey, and P. Mayewski, 1997, Electrical measurements on the Greenland Ice Sheet Project 2 Core, *Journal of Geophysical Research*, 102 (C12), 26511-26517.

Tegen, I., and I. Fung, 1994, Modeling of mineral dust in the atmosphere: Sources, transport, and optical thickness, *Journal of Geophysical Research*, 99 (D11), 22897-22914.

Wolff, G. T., 1984, On the nature of nitrate in coarse continental aerosols, *Atmospheric Environment*, 18 (5), 977-981.

Wurzler, S., T. G. Reisin, and Z. Levin, 2000, Modification of mineral dust particles by cloud processing and subsequent effects on drop size distributions, *Journal of Geophysical Research*, 105 (D4), 4501-4512.

FIGURES AND TABLE S

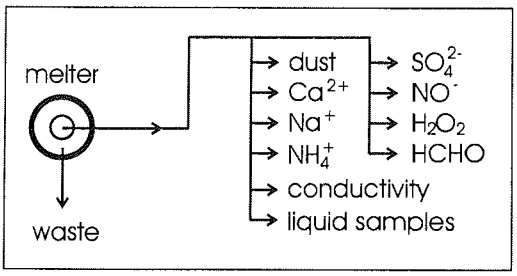

Figure 1. Flowchart of the analytical setup (highly simplified).

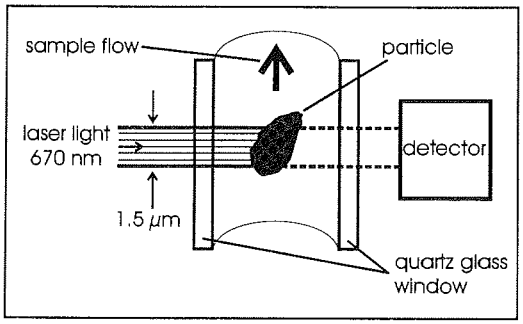

Figure 2. Detection cell of the laser sensor (schematic). The cross section of the cell is 230 µm × 250µm; the laser beam is 250 µm × 1.5 µm wide.

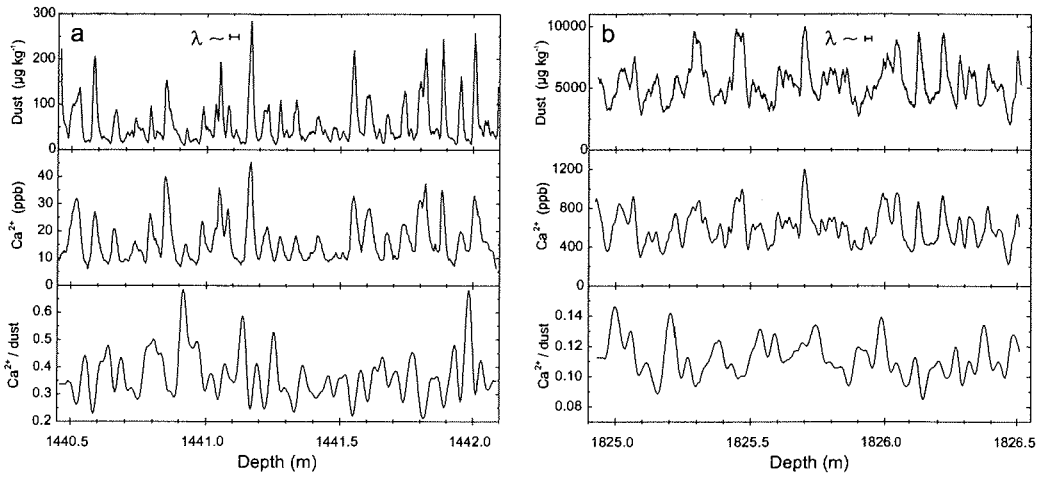

Figure 3. Examples of the insoluble dust and the Ca^{2+} measurements: (a) is in Holocene, (b) is during LGM. Also shown is the Ca^{2+}/dust ratio, which is smoothed (see text). A preliminary estimate of annual layer thicknesses λ is included. Note the different scales in all panels for (a) and (b).

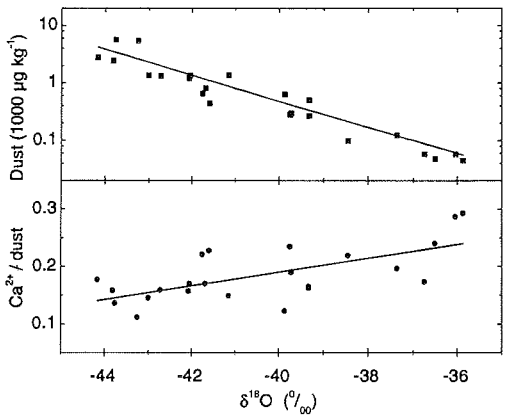

Figure 4. Ca^{2+}/dust ratio and mean dust concentration for all 23 sections plotted against $\delta^{18}O$. Each data point represents a 1.65 m long intervall.

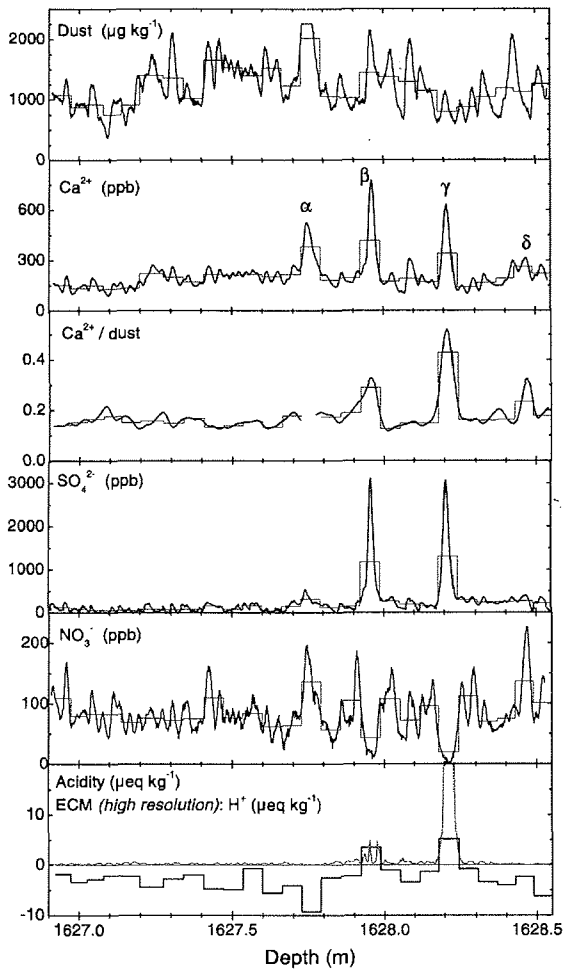

Figure 5. Examples of anomalous events in the microparticle and Ca^{2+} profiles. The sample is from the cold stadial between IS 1 and 2. The data for dust, Ca^{2+}, SO_4^{2-}, and NO_3^- were obtained by CFA; the Ca^{2+}/dust ratio was smoothed (see text); acidity was measured at approx. 6 cm depth resolution; in the same panel the ECM data is shown in high resolution (preliminary calibration). The fine histogram style lines represent the high resolution data reduced to the resolution of the acidity measurement. Labeled Ca^{2+} peaks refer to events discussed in text.

mid-depth (m)	climatic period	$\delta^{18}O$ (‰)	mean dust ($\mu g\ kg^{-1}$)	mean Ca^{2+}/ mean dust	unusual Ca^{2+}/dust	ECM peak	SO_4^{2-} peak
1424.8	hol	-35.87	44	0.29	-	na	-
1441.3	hol	-36.04	57	0.29	-	na	-
1459.4	hol	-36.74	58	0.17	+	na	+
1479.2	hol	-38.45	99	0.22	-	na	+
1486.9	hol	-36.60	48	0.24	-	na	-
1627.7	c-1/2	-42.07	1200	0.16	+	+	+
1642.6	c-1/2	-42.05	1347	0.17	+	+	+
1688.8	c-1/2	-42.73	1318	0.16	+	+	+
1716.8	c-1/2	-41.15	1353	0.15	+	+	+
1805.9	LGM	-43.76	5589	0.14	-	-	+
1825.7	LGM	-43.25	5373	0.11	-	-	-
1855.4	LGM	-43.00	1337	0.14	+	+	+
1895.0	c-4/5	-44.16	2755	0.18	-	-*	+
1931.3	c-4/5	-43.82	2418	0.16	+	+	+
2252.5	IS13	-41.59	440	0.23	+	+	+
2254.2	IS13	-39.75	280	0.23	+	+	+
2390.0	IS16	-39.72	298	0.19	+	+	+
2399.9	c-16/17	-41.68	810	0.17	-	-*	+
2708.5	c-21/22	-41.76	650	0.22	+	-	+
2901.5	c-pre23	-39.86	634	0.12	-	-	-
2904.8	c-pre23	-39.32	502	0.16	+	-	+
2918.0	w-23/5e1	-37.34	122	0.20	-	-	-
2921.3	c-post5e1	-39.32	268	0.16	+	-	+

Table. 1. Overview of the NGRIP core sections used for this study. All sections are 1.65 m long. The climatic period is preliminary; it was determined by matching the NGRIP dust profile to the GRIP $\delta^{18}O$ profile (Johnson and others, 1997). The NGRIP $\delta^{18}O$ values given are from personal communication from NGRIP members (2000). hol: Holocene; IS n: GRIP interstadial n; c m/n: cold stadial between SI m and SI n; LGM: last glacial maximum; pre23c: cold stage before IS23; w23/5e1: intermittent warm stage between IS23 and 5e1; post5e1: cold stage after 5e1. na: data not available; '+': existing; '-': not existing; '-': no ECM peak observed but a visible ash layer.*

Mean crust (igneous rocks)	0.041
Mean sediment	0.066
Marine carbonates	0.203
Mean limestone	0.340
Soils	0.015 (0.0007 – 0.50)

Table. 2. Mean weight fractions of Ca in different types of crust material (adapted from Bowen, 1978).